Role of (α, n) reactions under r-process conditions in neutrino-driven winds reexamined

Peter Mohr*
Diakonie-Klinikum, D-74523 Schwäbisch Hall, Germany
and Institute for Nuclear Research (ATOMKI), H-4001 Debrecen, Hungary
(Received 15 April 2016; published 7 September 2016)

Background: The astrophysical r-process occurs in an explosive astrophysical event under extremely neutron-rich conditions, leading to (n,γ)-(γ,n) equilibrium along isotopic chains which peaks around neutron separation energies of a few MeV. Nuclei with larger Z are usually produced by β^- decay, but under certain conditions also α-induced reactions may become relevant for the production of nuclei with $Z+2$.
Purpose: The uncertainties of the reaction rates of these α-induced reactions are discussed within the statistical model. As an example, α-induced (α,n) and (α,xn) reaction cross sections for the neutron-rich ^{86}Se nucleus are studied in detail.
Method: In a first step, the relevance of (α,n) and (α,xn) reactions is analyzed. Next the uncertainties are determined from a variation of the α-nucleus potential which is the all-dominant parameter for the astrophysical $Z \rightarrow Z+2$ reaction rate.
Results: It is found that the r-process flow towards nuclei with larger Z is essentially influenced only by the α-nucleus potential whereas the other ingredients of the statistical model play a very minor role. This finding is based on the fact that the flow towards larger Z depends on the sum over all (α,xn) cross sections, which is practically identical to the total α-induced reaction cross section.
Conclusions: α-nucleus potentials play an important role under certain r-process conditions because the flow towards larger Z depends sensitively on the total α-induced reaction cross section. The uncertainty of the reaction rate is about a factor of two to three at higher temperatures and exceeds one order of magnitude at very low temperatures.

DOI: 10.1103/PhysRevC.94.035801

I. INTRODUCTION

The astrophysical r-process is considered to be responsible for the nucleosynthesis of about one half of the nuclei heavier than iron. In a classical view, under the extremely neutron-rich r-process conditions with neutron densities above 10^{20}/cm^3, matter is driven towards neutron-rich nuclei by (n,γ) reactions. An equilibrium is established between (n,γ) and (γ,n) reactions for nuclei with low neutron binding energies of the order of a few MeV. Here the r-process flow has to wait for the much slower β^- decay to proceed towards nuclei with larger Z (so-called waiting-point approximation) [1–3].

It is obvious that the extreme conditions for the r-process can only be achieved in explosive scenarios. However, the astrophysical site(s) of the r-process are still under debate. The present study focuses onto the particular conditions which are found in neutrino-driven winds above a nascent neutron star or after the merging of two neutron stars. Here light r-process elements may be formed at high temperatures in a very short time scale of the order of milliseconds. Under these conditions the β^- decays may be too slow, and thus nuclei with larger Z can also be produced in a different way (e.g., Refs. [4–17]). The best candidate are α-induced reactions in the so-called α-process. These reactions are often somewhat simplisticly discussed as (α,n) reactions. However, the following analysis will show that not only the $(\alpha,1n)$, but also (α,xn) reactions may contribute and that the flow towards nuclei with larger Z is governed by the total α-induced reaction cross section σ_{reac}.

Very recently, a sensitivity study on the theoretical uncertainties of (α,n) reactions has been published by Pereira and Montes [17]. For the example of the ^{86}Se$(\alpha,n)^{89}$Kr reaction it was shown in Ref. [17] that the $(\alpha,1n)$ reaction rate is uncertain by at least an order of magnitude at low temperatures below $T_9 \approx 3$ (with T_9 being the temperature in 10^9 K), which is mainly based on the uncertainty which results from the choice of the α-nucleus potential. At higher temperatures above $T_9 \approx 5$ the uncertainty from the chosen α-nucleus potential reduces to about a factor of two to three, and the other ingredients of the statistical model calculations lead to similar uncertainties (see Fig. 6 of Ref. [17]). Furthermore, it is noticed in Ref. [17] that the widely used code NON-SMOKER [18] provides inclusive (α,n) cross sections and rates, whereas the open-source code TALYS [19] calculates also exclusive (α,xn) cross sections and rates. It is shown for the chosen example of ^{86}Se that the $(\alpha,1n)$ rate dominates at temperatures below $T_9 \approx 3$, whereas above $T_9 \approx 4$ the $(\alpha,2n)$ rate exceeds the $(\alpha,1n)$ rate significantly (Fig. 3 of Ref. [17]). As ^{86}Se is an unstable neutron-rich nucleus four mass units "east" of the heaviest stable selenium isotope ^{82}Se, the measurement of α-induced cross sections for ^{86}Se is extremely difficult, and up to now experimental data are not available.

The present study fully agrees with the discussion of the astrophysical scenario in Ref. [17] and the conclusion on the importance of the α-nucleus potential. In addition to Ref. [17], this work attempts to provide a better understanding of the uncertainties of α-induced reaction rates for the given astrophysical α-process scenario. For this purpose the following questions have to be addressed. (i) What is the astrophysically

*widmaiermohr@t-online.de

relevant quantity? (ii) How does this quantity depend on the underlying ingredients of the statistical model? (iii) Is there a deeper understanding of the corresponding nuclear physics? These questions will be answered in the following.

II. THE RELEVANT REACTIONS: (α,n) or (α,xn)?

For simplicity and better readability, the following discussion uses the example of ^{86}Se which was also chosen in Ref. [17]. It is pointed out in Ref. [17] that the (n,γ) and (γ,n) reactions are faster than other reactions by several orders of magnitude, thus leading to an equilibrium isotopic distribution (e.g., within the selenium isotopic chain) which is a function of temperature and neutron density. Let us assume that this isotopic distribution peaks at ^{86}Se. Following the approximation given in Eq. (25) of Ref. [2], this corresponds, e.g., to $T_9 = 3$ and $N_n \approx 10^{24}/\mathrm{cm}^3$. Then the flow towards larger Z may proceed via $^{86}\mathrm{Se}(\alpha,1n)^{89}\mathrm{Kr}$, or in general via $^{86}\mathrm{Se}(\alpha,xn)^{90-x}\mathrm{Kr}$ (with $x = 1, 2, 3$, etc.). Even the case $x = 0$, i.e., the $^{86}\mathrm{Se}(\alpha,\gamma)^{90}\mathrm{Kr}$ reaction, may contribute although the (α,γ) cross section is typically much smaller than the (α,xn) cross sections.

As soon as any krypton isotope is made in this way, the fast (n,γ) and (γ,n) reactions drive krypton immediately towards ^{90}Kr, which has a neutron separation energy similar to ^{86}Se. This conclusion is completely independent of the production by $(\alpha,1n)$ or (α,xn) reactions, i.e., independent whether krypton is made as ^{86}Kr or ^{90}Kr. In general, (n,γ) rates increase with increasing positive (n,γ) Q value towards less neutron-rich nuclei, i.e., towards stability. Thus, e.g., ^{86}Kr from the $^{86}\mathrm{Se}(\alpha,4n)^{86}\mathrm{Kr}$ reaction is very efficiently transmuted to ^{90}Kr by a fast series of (n,γ) reactions.

From the above arguments it becomes evident that the astrophysically relevant quantity is the total production of Kr isotopes by (α,xn) reactions, i.e., the sum over $(\alpha,1n)$, $(\alpha,2n)$, $(\alpha,3n)$, etc., including also the weak (α,γ) cross section. For the typical temperatures of the α-process [17], the total reaction cross section for the chosen example of ^{86}Se is governed by the $(\alpha,1n)$ channel. The reaction rate of the $(\alpha,2n)$ channel contributes only minor amounts because of the negative Q value of about -4.5 MeV, and the reaction rates of the $(\alpha,3n)$ and $(\alpha,4n)$ channels are practically negligible.

III. TOTAL α-INDUCED REACTION CROSS SECTION σ_{reac} AND THE α-NUCLEUS POTENTIAL

The total reaction cross section σ_{reac} of α-induced reactions is given by the sum over all open reaction channels. In the case of neutron-rich nuclei, any proton emission is highly suppressed because of the negative Q value. In the given example of ^{86}Se the Q value of the (α,p) reaction is about -7 MeV, and thus the astrophysical reaction rate $N_A\langle\sigma v\rangle$ of the (α,p) reaction remains negligibly small. As a consequence, the total reaction cross section σ_{reac} is practically identical to the sum over the cross sections of the neutron-emitting (α,xn) channels which has been identified as the astrophysically relevant quantity in Sec. II. A minor contribution of inelastic (α,α') scattering to the total reaction cross section σ_{reac} typically remains far below 10 % at astrophysically relevant energies [20].

The total reaction cross section σ_{reac} is related to the reflexion coefficients η_L by

$$\sigma_{\mathrm{reac}} = \frac{\pi}{k^2}\sum_L (2L+1)\left(1-\eta_L^2\right) \qquad (1)$$

with the angular momentum L and the wave number $k = \sqrt{2\mu E}/\hbar$, E the energy in the center-of-mass system, and the reduced mass μ of α projectile and target. From a given α-nucleus potential, the reflexion coefficients η_L and phase shifts δ_L can be calculated by solving the Schrödinger equation. As the total reaction cross section σ_{reac} depends only on the η_L in Eq. (1), σ_{reac} depends only the the chosen α-nucleus potential, but not on the other ingredients of statistical model calculations. A general behavior of the η_L will be discussed in the subsequent Sec. IV. First I extend the sensitivity study of Ref. [17] by including additional α-nucleus potentials. In particular, I include the recent many-parameter potential by Avrigeanu and coworkers (in the version of Ref. [21]), the few-parameter ATOMKI-V1 potential [22], and the modified McFadden-Satchler potential as suggested by Sauerwein *et al.* [23]. I compare the results to the TALYS v1.6 default potential, which is based on Ref. [24] and to the α-nucleus potentials of McFadden and Satchler [25] and three different versions suggested by Demetriou *et al.* [26]. The latest global α-nucleus potential by Su and Han [27] has not been optimized for energies below the Coulomb barrier, and it has been found in Ref. [20] that it overestimates the experimental total reaction cross section σ_{reac} of ^{64}Zn at low energies significantly. In the present case of ^{86}Se, σ_{reac} is also much higher by a factor of about 2 at 10 MeV and more than one order of magnitude at 5 MeV. The results from the potential of Ref. [27] are thus omitted in Fig. 1.

Whereas the uncertainty study of Ref. [17] discusses reaction rates, the present work will compare the underlying cross sections. Here it will become visible that at higher energies all predictions of σ_{reac} from the different α-nucleus potentials agree within about 10% whereas dramatic discrepancies are found at very low energies. For completeness it has to be pointed out that the calculated cross sections in the present work are calculated under laboratory conditions, i.e., without thermal excitations of the ^{86}Se target nucleus. However, for the case of ^{86}Se, stellar enhancement factors remain close to unity up to temperatures of about $T_9 \approx 5$ [18].

The results for the different α-nucleus potentials [21–26] are shown in Fig. 1. Because the cross sections cover many orders of magnitude, the lower part of Fig. 1 shows in addition the ratio normalized to the widely used McFadden-Satchler potential. It has been shown recently that this potential provides an excellent description of α-induced reaction cross sections for relatively light nuclei in the $A \approx 20$–50 mass range [28] whereas for heavier targets the McFadden-Satchler potential tends to overestimate the cross sections, in particular at low energies below the Coulomb barrier. Note that the folding potential in the three versions of the Demetriou *et.* [26] potential is calculated within the TALYS code, whereas the folding potential of the ATOMKI-V1 potential was derived

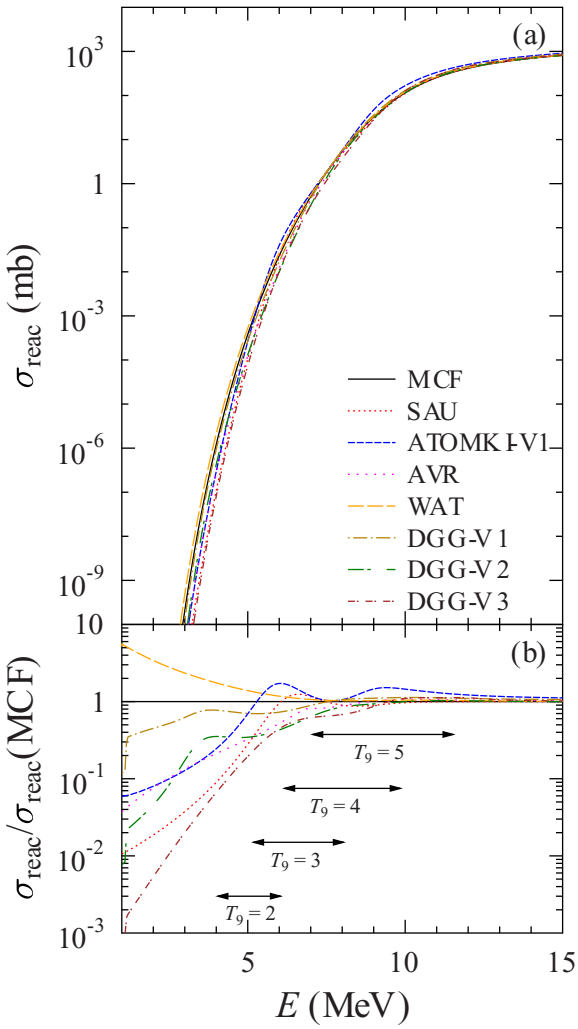

FIG. 1. Total reaction cross section σ_{reac} for α-induced reactions on ^{86}Se, calculated from different α-nucleus potentials: McFadden and Satchler (MCF) [25], Sauerwein *et al.* (SAU) [23], ATOMKI-V1 [22], Avrigeanu *et al.* (AVR) [21], Watanabe (WAT; TALYS default) [24], and Demetriou *et al.* (DGG): versions 1–3 from Ref. [26]. The upper part (a) shows the cross sections, which cover many orders of magnitude. The lower part (b) shows the ratio normalized to the widely used McFadden-Satchler potential. The Gamow window for temperatures $T_9 = 2$–5 is indicated by horizontal arrows. For further discussion see the text.

from a 2-parameter Fermi distribution for ^{86}Se and average parameters of neighboring nuclei given in Ref. [29].

At higher energies above 15 MeV the predictions from all α-nucleus potentials under study agree within about 10%. This is an expected behavior as will be shown in Sec. IV. However, at lower energies significant discrepancies can be found. Between 7 and 10 MeV (corresponding to the Gamow windows around $T_9 \approx 4$–5) the predictions show a variation of about a factor of two to three. At even lower energies around 5 MeV (corresponding to the Gamow window at $T_9 \approx 2$) the uncertainty exceeds one order of magnitude. At very low energies, the range of predicted σ_{reac} exceeds two orders of magnitude. It should be noted that σ_{reac} is very small, of the order of 10^{-20} mb (10^{-12} mb) at $E = 2$ MeV (3 MeV). Fortunately, it is found that the numerical results from two independent codes with slightly different default settings (TALYS, which uses ECIS [30] as subroutine for σ_{reac}, and A0 [31]) agree within a few percent down to such tiny cross sections; this discrepancy is further reduced as soon as identical settings are chosen in both codes.

Figure 1(a) shows the huge variation of σ_{reac} with energy which results from the Coulomb barrier. Figure 1(b) visualizes that all α-nucleus potentials under study agree very well at energies above 15 MeV, whereas the range of predicted σ_{reac} increases dramatically towards lower energies below the Coulomb barrier. The range of predictions for the astrophysical reaction rate $N_A\langle\sigma v\rangle$ can be estimated for temperatures of $T_9 = 2$–5 from the marked Gamow windows. Compared to the previous study [17], this range of predictions is somewhat increased because three additional α-nucleus potentials have been studied in this work.

The usual calculation of the Gamow window energies is based on the simplistic assumption of a constant astrophysical S factor which is not realistic for heavy nuclei. Nevertheless, the Gamow window provides still a reasonable estimate for the most relevant energy region for the astrophysical reaction rate. Because the astrophysical S factor typically decreases with increasing energy for α-induced reactions on heavy target nuclei, this leads to a shift of the most effective energy towards lower energies by typically about 1 MeV; for a detailed discussion of this shift, see Ref. [32].

IV. GENERAL BEHAVIOR OF REFLEXION COEFFICIENTS η_L

The total reaction cross section σ_{reac} depends on the reflexion coefficients η_L; see Eq. (1). It has already been discussed in detail [33,34] that there is a general behavior of the η_L at energies above the Coulomb barrier. Partial waves with small angular momentum L (corresponding to small impact parameters or central collisions in a semiclassical view) are practically fully absorbed ($\eta_L \approx 0$), and partial waves with large L (large impact parameters, peripheral trajectories) are not absorbed ($\eta_L \approx 1$).

The transition from $\eta_L \approx 0$ to $\eta_L \approx 1$ happens within few partial waves; consequently, the differences between any realistic potentials are restricted to these few partial waves with $\eta_L \gg 0$ and $\eta_L \ll 1$, and the resulting total reaction cross section σ_{reac} is relatively well defined as long as the chosen potential has a reasonable radial range and a sufficient absorptive strength. In the chosen example of $\alpha+^{86}$Se this behavior holds down to about 15 MeV, where the relevant angular momentum number range is $5 \lesssim L \lesssim 10$ (see Fig. 2), leading to uncertainties for σ_{reac} of less than 10 % above 15 MeV.

The following discussion and presentation in Fig. 2 will focus on the widely used McFadden-Satchler potential (MCF) [25], the many-parameter potential by Avrigenau *et al.* (AVR) [21], and the ATOMKI-V1 potential [22]. The total reaction cross sections σ_{reac} at the energies of Fig. 2 are listed in Table I.

At 15.0 MeV, total reaction cross sections σ_{reac} between 812 and 908 mb are found for the potentials [21–26]. Obviously,

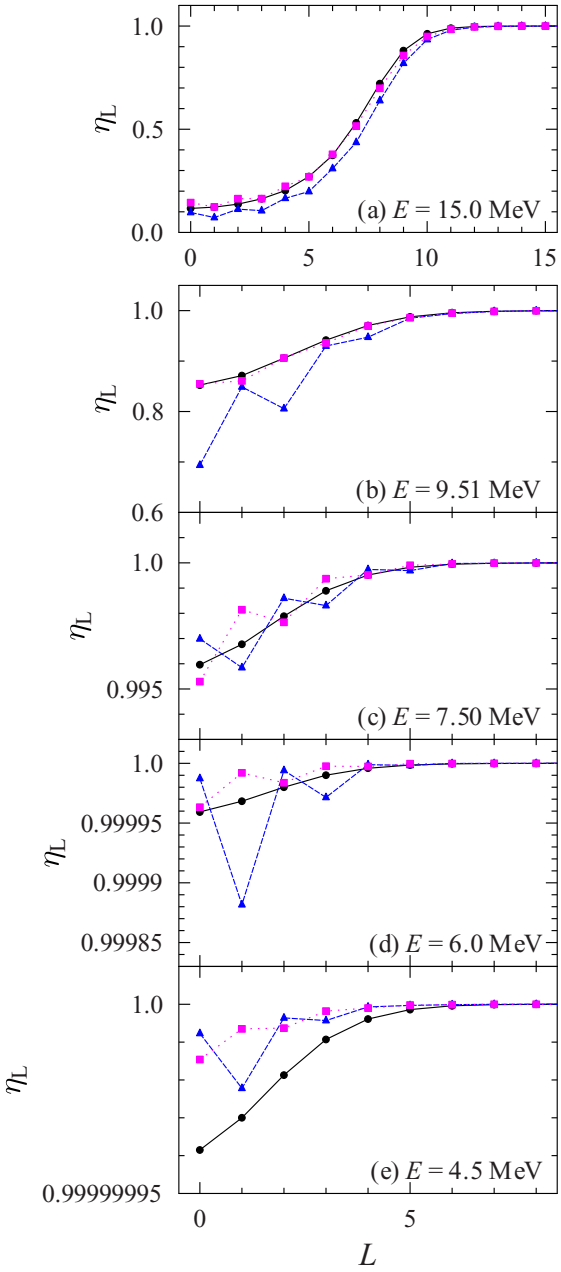

FIG. 2. Reflexion coefficients η_L at different energies above, around, and below the Coulomb barrier, calculated from the potentials of McFadden-Satchler [25] (black circles), Avrigeanu *et al.* [21] (magenta squares), and ATOMKI-V1 [22] (blue triangles). The corresponding total reaction cross sections $\sigma_{\rm reac}$ from Eq. (1) are listed in Table I. At the highest energy of 15 MeV (a), η_L for partial waves $L = 0$–15 are shown; here $\eta_L \approx 0$ for small L and $\eta_L \approx 1$ for $L \gtrsim 10$. All potentials under study predict this generic behavior above the Coulomb barrier. At lower energies [(b)–(e)] the η_L are shown for $L = 0$–8. Here only the η_L for these few partial waves deviate from unity and thus contribute to the sum for $\sigma_{\rm reac}$ in Eq. (1). Now the calculated η_L depend sensitively on the properties of the α-nucleus potentials. Note the extremely different scales for η_L in panels (a)–(e), with the tiny deviations smaller 5×10^{-8} from unity at the lowest energy (e). The data points are connected by thin lines to guide the eye. Color codes and line styles are identical to Fig. 1. For further discussion see the text.

TABLE I. Predictions of $\sigma_{\rm reac}$ from various global α-nucleus potentials [21,22,25], corresponding to the η_L shown in Fig. 2.

E (MeV)	$\sigma_{\rm reac}$(b)		
	AVR Ref. [21]	ATOMKI-V1 Ref. [22]	MCF Ref. [25]
15.0	8.39×10^{-1}	9.08×10^{-1}	8.13×10^{-1}
9.51	6.95×10^{-2}	9.98×10^{-2}	6.59×10^{-2}
7.50	1.49×10^{-3}	1.86×10^{-3}	1.80×10^{-3}
6.0	1.08×10^{-5}	3.61×10^{-5}	2.11×10^{-5}
4.5	0.69×10^{-8}	1.02×10^{-8}	2.65×10^{-8}

the largest deviations of the η_L from unity are found for the ATOMKI-V1 potential in Fig. 2(a), and thus, according to Eq. (1), the ATOMKI-V1 potential leads to a slightly larger $\sigma_{\rm reac}$ of 908 mb whereas the MCF (813 mb) and the AVR (839 mb) predictions are quite close to each other. Overall, the deviations between the different potentials remain quite limited with about 10%.

The situation changes dramatically towards lower energies. Some further energies were selected for illustration in Fig. 2 where interesting properties can be seen for the cross-sectional ratios in Fig. 1. In general, at lower energies full absorption ($\eta_L \approx 0$) is not reached for any partial wave. At energies far below the Coulomb barrier all η_L approach unity, and the total reaction cross section is given by the tiny deviation of the η_L from unity for very few partial waves with small $L \lesssim 5$. These tiny deviations depend sensitively on the chosen α-nucleus potential.

At $E = 9.51$ MeV the ATOMKI-V1 potential predicts a cross section which is a factor of about 1.5 above the MCF and AVR predictions. Interestingly, this is related to a relatively strong absorption of the even partial waves with $L = 0$ and $L = 2$, whereas the η_L for the odd partial waves are almost identical for all potentials; see Fig. 2(b).

At $E = 7.50$ MeV the three potentials under study provide almost identical $\sigma_{\rm reac}$. However, this agreement must be considered at random. The MCF potential shows a smooth L dependence, the AVR potential shows stronger absorption for even L, and the ATOMKI-V1 potential favors absorption for odd L; see Fig. 2(c).

This odd-even staggering becomes more pronounced at $E = 6.0$ MeV. Here the strong absorption of the $L = 1$ partial wave leads to an ATOMKI-V1 cross section which is about a factor of two above the MCF potential and a factor of three above the AVR potential; see Fig. 2(d).

At the lowest energy of $E = 4.5$ MeV in Fig. 2(e) $\sigma_{\rm reac}$ from the MCF potential is about a factor of 2–3 above the predictions from the ATOMKI-V1 and AVR potentials. Towards even lower energies, the predictions of ATOMKI-V1 and AVR agree surprisingly well, whereas MCF predicts much larger cross sections. Again, the relatively good agreement between ATOMKI-V1 and AVR must be considered as accidental because of the discrepant underlying η_L from the ATOMKI-V1 and AVR potentials.

The odd-even staggering of the η_L for the ATOMKI-V1 and AVR potentials results directly from the numerical solution of the Schrödinger equation. In both potentials the imaginary

part is dominated by a surface Woods-Saxon potential, i.e., absorption within a limited radial range. Thus, the absorption becomes sensitive to the details of the wave function for each partial wave. The different radius parameters ($R_S = 1.43$ fm for ATOMKI-V1, 1.52 fm for AVR; to be multiplied by $A_T^{1/3}$) lead to the different behavior of the η_L at the low energies in Fig. 2. The odd-even staggering is more pronounced for the ATOMKI-V1 potential with its pure surface absorption, whereas the AVR potential includes also a small-volume Woods-Saxon imaginary potential at low energies. The odd-even staggering does practically not appear for the MCF potential with its pure volume Woods-Saxon imaginary part.

V. DISCUSSION

A. Cross sections

The calculations of the total reaction cross section $\sigma_{\rm reac}$ in Fig. 1 and the underlying reflexion coefficients η_L in Fig. 2 show that $\sigma_{\rm reac}$ is relatively well defined within about a factor of two to three down to about 8 MeV. This covers the Gamow windows above $T_9 \approx 4$. At lower energies down to about 5 MeV, corresponding to Gamow windows for the temperatures around $T_9 \approx 2$–3, the uncertainty increases and reaches about one order of magnitude.

Recently, it has been found that so-called reduced cross sections and reduced energies (as suggested in Ref. [35]) can be used to compare α-induced cross sections for many targets over a wide range of energies [28]. The reduced energy $E_{\rm red}$ and the reduced cross section $\sigma_{\rm red}$ are defined by

$$E_{\rm red} = \frac{\left(A_P^{1/3} + A_T^{1/3}\right) E_{\rm c.m.}}{Z_P Z_T}, \tag{2}$$

$$\sigma_{\rm red} = \frac{\sigma_{\rm reac}}{\left(A_P^{1/3} + A_T^{1/3}\right)^2}. \tag{3}$$

At reduced energies above $E_{\rm red} \approx 1.5$ MeV all nuclei show very similar $\sigma_{\rm red}$ values of the order of 20–50 mb. Towards lower energies, the Coulomb barrier leads to decreasing $\sigma_{\rm red}$. Figure 3 shows experimental results for heavier ($A \gtrsim 90$) targets with blue crosses; because the results remain very similar, the same symbol has been chosen (for details see Refs. [22,36]). The $\sigma_{\rm red}$ for lighter targets are somewhat larger than for heavier targets; experimental results are shown for ^{64}Zn, ^{50}Cr, ^{44}Ti, and ^{34}S (taken from Ref. [28]). The predictions from eight different α-nucleus potentials [21–26] for the neutron-rich ^{86}Se nucleus are shown as lines; these predictions fit nicely into the general systematics in Fig. 3.

The various potentials [21–26] have been determined from experimental data for stable nuclei. Obviously, an extrapolation of the parameters is needed for the α-nucleus potential of the neutron-rich ^{86}Se nucleus. The good agreement of the different predictions at higher $E_{\rm red}$ gives some confidence into this extrapolation but unfortunately cannot further constrain the low-energy cross section and the astrophysical reaction rate. Note that there is an approximate relation between reduced energies and the Gamow window [37]: $E_{\rm red,0} \approx 0.284\,{\rm MeV} \times T_9^{2/3}$. Consequently, the astrophysically relevant range for the reduced energy $E_{\rm red}$ is located below the shown range of Fig. 3 which was chosen from the availability of experimental data (taken from Refs. [22,28]).

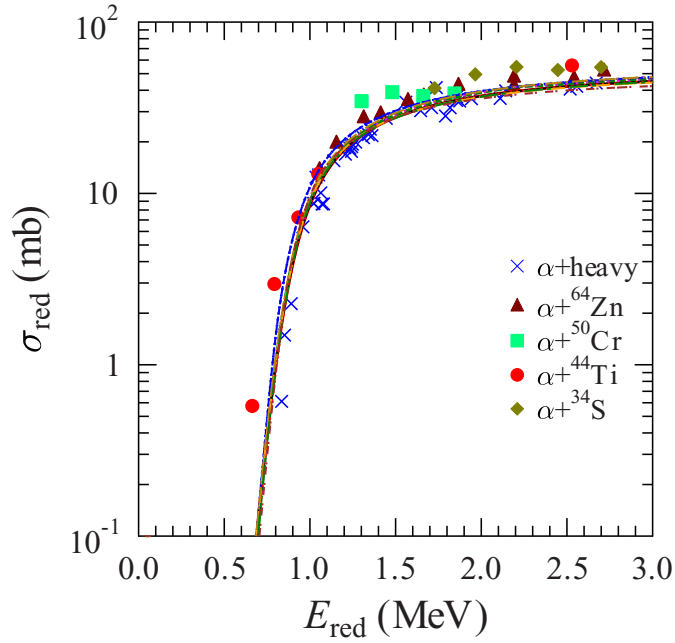

FIG. 3. Reduced cross sections $\sigma_{\rm red}$ vs reduced energy $E_{\rm red}$ for heavy ($A \gtrsim 90$) and some lighter target nuclei (experimental data taken from Refs. [22,28]). The predictions for ^{86}Se from the different potentials [21–26] are shown with lines; they are relatively close (within a factor of two to three) for $E_{\rm red}$ above 0.7 MeV (corresponding to $E \approx 8$ MeV), and thus the different lines appear as almost identical in the logarithmic scale. Color codes and line styles are identical to Fig. 1.

The above analysis of α-induced reactions on ^{86}Se and the role of (α,n) and (α,xn) reactions can be extended to a broader range of target nuclei. The general conclusions on the behavior of the η_L will remain valid, and the resulting uncertainties of $\sigma_{\rm reac}$ for a wider range of targets will be quite similar to the chosen example of ^{86}Se.

B. Consequences for astrophysical reaction networks

It has been shown above that the astrophysically relevant quantity for the production of nuclei with $Z+2$ under r-process conditions is the sum over all (α,xn) cross sections which can be approximated by the total reaction cross section $\sigma_{\rm reac}$. As a consequence, the astrophysical reaction rate depends only on the α-nucleus potential, but is insensitive to the other ingredients of the statistical model calculations. Although the other ingredients do affect the branching ratios into the different $(\alpha,1n)$, $(\alpha,2n)$, $(\alpha,3n)$, etc. channels; they do not affect the total cross section $\sigma_{\rm reac}$.

Compared to the recent study of Pereira and Montes [17] where uncertainties for the $(\alpha,1n)$ rate were estimated from all ingredients of the statistical model, the present approach should in principle lead to smaller uncertainties which are exclusively based on the uncertainty of the α-nucleus potential. However, such a reduction of uncertainties is only found at very high temperatures where the $(\alpha,2n)$ and $(\alpha,3n)$ channels

contribute significantly; such high temperatures exceed the typical range of the α-process as discussed in Ref. [17]. At typical α-process temperatures below $T_9 \approx 3$, the $(\alpha,1n)$ channel is dominating the total reaction cross section $\sigma_{\rm reac}$. Consequently, also in Ref. [17] the α-nucleus potential was identified as the dominating source of uncertainties. The present study finds even a slightly increased uncertainty for the reaction rate at low temperatures from the larger range of predictions from the three additionally considered α-nucleus potentials [21,23,28].

Extended astrophysical reaction networks should include all (α,xn) reactions and their predicted rates, e.g., from the TALYS code. As pointed out in Ref. [17], the inclusive (α,n) rates from the NON-SMOKER code may induce errors if they are considered as exclusive $(\alpha,1n)$ rates in such an extended reaction network. However, this error remains small as long as the (n,γ)-(γ,n) equilibrium is established sufficiently fast and smears out the produced isotopic distribution from the different (α,xn) reactions. On the contrary, a significant error will occur as soon as a limited reaction network which includes only the $(\alpha,1n)$, but not the (α,xn), channels is fed by the exclusive $(\alpha,1n)$ rate, e.g., from TALYS; here the flow towards nuclei with larger Z will be underestimated. Finally, it should be noted that the limited reaction network will do a good job again using inclusive (α,n) rates of NON-SMOKER or TALYS.

Unfortunately, with the exception of Ref. [6], none of Refs. [2–5,7–16] state explicitly whether the chosen network considers the different (α,xn) channels. The widely used REACLIB database [38] contains for the chosen example of $\alpha+^{86}$Se only the (α,γ), (α,n), and (α,p) rates. (α,xn) rates are not included in REACLIB. Thus, it seems very likely that most of the r-process network calculations use limited networks without explicit consideration of the (α,xn) channels. As REACLIB recommends the inclusive rates from NON-SMOKER, the final results should not be affected dramatically by this limitation.

VI. CONCLUSIONS

Very recently, Pereira and Montes [17] have shown that $(\alpha,1n)$ reaction rates depend sensitively on the chosen α-nucleus potential at low temperatures and show a weaker dependence on further ingredients of the statistical model at higher temperatures. This finding is correct for the exclusive $(\alpha,1n)$ rate. However, the present study shows that the astrophysically relevant rate, i.e., the production of a nucleus with $Z+2$ by (α,xn) reactions under r-process conditions, is essentially defined by the sum over all (α,xn) rates which is approximately given by the total α-induced reaction cross section $\sigma_{\rm reac}$. This finding is based on the rapid establishment of an equilibrium isotopic distribution by (n,γ) and (γ,n) reactions, which is independent of the particular (α,xn) production reaction. As the total reaction cross section $\sigma_{\rm reac}$ depends only on the underlying α-nucleus potential, but not on the other ingredients of the statistical model, the uncertainty of the astrophysical rate can be well estimated from the uncertainty of the α-nucleus potential only.

It is found that the uncertainty of $\sigma_{\rm reac}$ at higher energies above 15 MeV is very small, whereas it increases dramatically towards lower energies. This leads to uncertainties of the reaction rate which are about a factor of two to three for higher temperatures of $T_9 \approx 4$–5 and about one order of magnitude for lower temperatures of $T_9 \approx 2$–3. At even lower temperatures the uncertainty increases further. Compared to the study in Ref. [17], the additional consideration of three recent α-nucleus potentials of Refs. [21,23,28] slightly increases the range of predicted $\sigma_{\rm reac}$ between 5 and 10 MeV. The different predictions of $\sigma_{\rm reac}$ result from different reflexion coefficients η_L which depend sensitively on the properties of the chosen α-nucleus potential at low energies below the Coulomb barrier. Interestingly, some cases have been identified where discrepant predictions of η_L lead to almost the same total reaction cross section $\sigma_{\rm reac}$ which is given by sum over all contributing partial waves. Any experimental test of the global α-nucleus potentials [21–26] for nuclei with extreme N/Z ratio is very desirable. Such experiments may come in reach with the upcoming radioactive ion beam facilities.

The astrophysical modeling of the r-process in an extended network (including all (α,xn) reaction channels) or in a limited network (with $(\alpha,1n)$ reactions only) has to be consistent with the definition of exclusive (α,xn) (e.g., from TALYS) or inclusive (α,n) cross sections and rates (as, e.g., provided by NON-SMOKER). The largest error occurs if a limited network is used in combination with the exclusive $(\alpha,1n)$ rate (e.g., from TALYS); in this case the r-process flow towards larger Z is underestimated because of the missing contributions from the (α,xn) rates (with $x > 1$). An extended network with the inclusive (α,n) rate (e.g., from NON-SMOKER) for the exclusive $(\alpha,1n)$ channel is not fully correct, but the (n,γ)-(γ,n) equilibrium will keep the resulting error relatively small.

ACKNOWLEDGMENTS

I thank Zs. Fülöp, Gy. Gyürky, and G. G. Kiss for many encouraging discussions on α-nucleus potentials, and J. Pereira and F. Montes for their constructive criticisms. This work was supported by OTKA (Grants No. K108459 and No. K120666).

[1] J. J. Cowan, F.-K. Thielemann, and J. W. Truran, Phys. Rep. **208**, 267 (1991).
[2] M. Arnould, S. Goriely, and K. Takahashi, Phys. Rep. **450**, 97 (2007).
[3] F.-K. Thielemann *et al.*, Prog. Part. Nucl. Phys. **66**, 346 (2011).
[4] S. Woosley and R. D. Hoffman, Astrophys. J. **395**, 202 (1992).
[5] K. Otsuki, H. Tagoshi, T. Kajino, and S. Wanajo, Astrophys. J. **533**, 424 (2000).
[6] S. Wanajo, T. Kajino, G. J. Mathews, and K. Otsuki, Astrophys. J. **554**, 578 (2001).

[7] M. Teresawa, K. Sumiyoshi, T. Kajino, G. J. Mathews, and I. Tanihata, Astrophys. J. **562**, 470 (2001).
[8] K. Sumiyoshi, M. Teresawa, G. J. Mathews, T. Kajino, S. Yamada, and H. Suzuki, Astrophys. J. **562**, 880 (2001).
[9] B. S. Meyer, Phys. Rev. Lett. **89**, 231101 (2002).
[10] Y.-Z. Qian and G. J. Wasserburg, Phys. Rep. **442**, 237 (2007).
[11] Y.-Z. Qian and G. J. Wasserburg, Astrophys. J. **687**, 272 (2008).
[12] K. Farouqi, K.-L. Kratz, B. Pfeiffer, T. Rauscher, F.-K. Thielemann, and J. W. Truran, Astrophys. J. **712**, 1359 (2010).
[13] A. Arcones and F. Montes, Astrophys. J. **731**, 5 (2011).
[14] A. Arcones and F.-K. Thielemann, J. Phys. G **40**, 013201 (2013).
[15] S. Goriely, Eur. Phys. J. **51**, 22 (2015).
[16] D. Martin, A. Perego, A. Arcones, F.-K. Thielemann, O. Korobkin, and S. Rosswog, Astrophys. J. **813**, 2 (2015).
[17] J. Pereira and F. Montes, Phys. Rev. C **93**, 034611 (2016).
[18] T. Rauscher, computer code NON-SMOKER [http://nucastro.org/nonsmoker.html].
[19] A. J. Koning, S. Hilaire, and S. Goriely, computer code TALYS [http://www.talys.eu].
[20] A. Ornelas, P. Mohr *et al.* (unpublished).
[21] V. Avrigeanu, M. Avrigeanu, and C. Manailescu, Phys. Rev. C **90**, 044612 (2014).
[22] P. Mohr, G. G. Kiss, Zs. Fülöp, D. Galaviz, Gy. Gyürky, and E. Somorjai, At. Data Nucl. Data Tables **99**, 651 (2013).
[23] A. Sauerwein, H. W. Becker, H. Dombrowski, M. Elvers, J. Endres, U. Giesen, J. Hasper, A. Hennig, L. Netterdon, T. Rauscher, D. Rogalla, K. O. Zell, and A. Zilges, Phys. Rev. C **84**, 045808 (2011).
[24] S. Watanabe, Nucl. Phys. **8**, 484 (1958).
[25] L. McFadden and G. R. Satchler, Nucl. Phys. **84**, 177 (1966).
[26] P. Demetriou, C. Grama, and S. Goriely, Nucl. Phys. A **707**, 253 (2002).
[27] X.-W. Su and Y.-L. Han, Int. J. Mod. Phys. E **24**, 1550092 (2015).
[28] P. Mohr, Eur. Phys. J. A **51**, 56 (2015).
[29] H. de Vries, C. W. de Jager, and C. de Vries, At. Data Nucl. Data Tables **36**, 495 (1987).
[30] J. Raynal, Saclay Report No. CEA-N-2772, 1994 (unpublished).
[31] H. Abele and P. Mohr, computer code A0, version 1.51, University Tübingen (unpublished).
[32] T. Rauscher, Phys. Rev. C **81**, 045807 (2010).
[33] P. Mohr, Phys. Rev. C **84**, 055803 (2011).
[34] P. Mohr, Phys. Rev. C **87**, 035802 (2013).
[35] P. R. S. Gomes, J. Lubian, I. Padron, and R. M. Anjos, Phys. Rev. C **71**, 017601 (2005).
[36] P. Mohr, D. Galaviz, Zs. Fülöp, Gy. Gyürky, G. G. Kiss, and E. Somorjai, Phys. Rev. C **82**, 047601 (2010).
[37] P. Mohr, Proceedings of the Nuclear Physics in Astrophysics VII, York, UK, 18–22 May 2015, J. Phys. Conf. Ser., arXiv:1608.08233 [nucl-th].
[38] R. H. Cyburt *et al.*, Astrophys. J. Suppl. **189**, 240 (2010); REACLIB database available at https://groups.nscl.msu.edu/jina/reaclib/db/.